2008 IEEE International Conference on
Robotics and Automation
Pasadena, CA, USA, May 19-23, 2008

Evolution of a Jump in an Articulated Leg with Series-Elastic Actuation

Simon Curran and David E. Orin
Department of Electrical and Computer Engineering
The Ohio State University
Columbus, OH 43210
Email: curran.62@osu.edu, orin.1@osu.edu

Abstract— **The remarkable ability of humans and animals to perform dynamic maneuvers, such as a jump, is largely attributed to series-elastic elements in skeletal muscle. Both the degree of elasticity and the coordination of muscular contractions have been shown to impact jump performance. The objective of this paper is to use a genetic algorithm (GA) to optimize the control and actuator parameters of a series-elastic actuator (SEA), which is functionally analogous to skeletal muscle, in an articulated leg to produce the highest jump. Similar to skeletal muscle, the control and stiffness of the SEA is found by the GA to affect jump performance, yielding solutions with biological properties. In particular, the jumps evolved by the GA made use of the stretch and shortening cycle of the series-elasticity, which is commonly seen in nature to increase the force of an explosive movement. The model studied in this paper is of a prototype leg with series-elastic actuation. A detailed leg and actuator model was developed to include the important electrical and mechanical properties of the DC motors as well as the characteristics of the motor amplifiers.**

Key words: dynamic maneuvers, jump, legged robot, series-elastic actuation (SEA), evolutionary robotics.

I. Introduction

The need for explosive leg power is essential if legged robots are going to be capable of performing dynamic maneuvers. Dynamic maneuvers, which give humans their agility, involve sudden changes in trajectory or speed. Typically, these maneuvers take the form of high-speed turning, dodging, jumping, and starting quickly. The sudden changes of trajectory, however, are associated with large accelerations that must be realized with explosive leg power. At present, actuator power is still a major limitation with legged machines; as such, dynamic maneuvers remain an elusive goal in the field of legged robotics.

In exercise physiology, the ability to perform powerful dynamic movements is attributed to the stretch and shortening cycle of muscles and tendons [1]. When a muscle lengthens as a result of an eccentric contraction, it stores elastic energy in the muscle's fibers and tendons. If followed immediately by a contraction, the additional stored energy is available to do more work and allows the muscle to shorten with a larger force. Numerous studies have shown that tendon elasticity plays an important role in enhancing muscle work output for a variety of movements [2], [3], [4], [5], [6], [7]. Furthermore, Bobbert found that the human squat jump performance was highly dependent upon the stiffness of the series-elastic elements of the legs [8]. Also, work done by Ettema showed that the timing of the muscle contractions was crucial for the effective release of energy stored in the series-elastic elements of skeletal muscle [9]. Biomimicry suggests that the series-elastic actuator (SEA), which has a similar series-elastic element, could benefit from the characteristics just described and will be addressed by this paper.

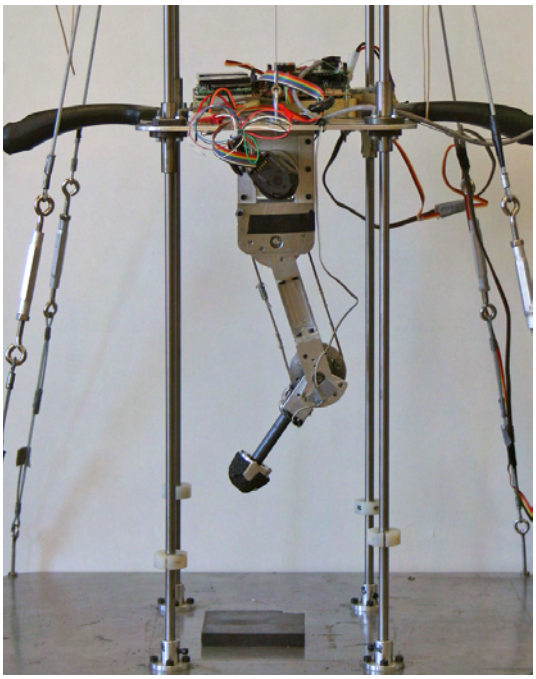

Fig. 1. Photograph of the prototype articulated leg on its vertical constraint rails.

This paper will study the light-weight articulated leg with series-elastic actuation shown in Fig. 1 developed by Remic [10], Curran [11], and Knox [12]. The leg has two actuators fixed to the body that actuate the hip and knee joints. The configuration is such that the leg is a two-link serially connected mechanism, where each link is actuated in parallel with respect to the body, through a cable-pulley transmission.

The response of an SEA during impulsive movements is highly nonlinear and difficult to model. Applying conventional control and optimization techniques to determine the crucial time to apply control inputs is generally not feasible. Yet, through trial and error, nature has shown the ability to discover or learn these optimum control inputs,

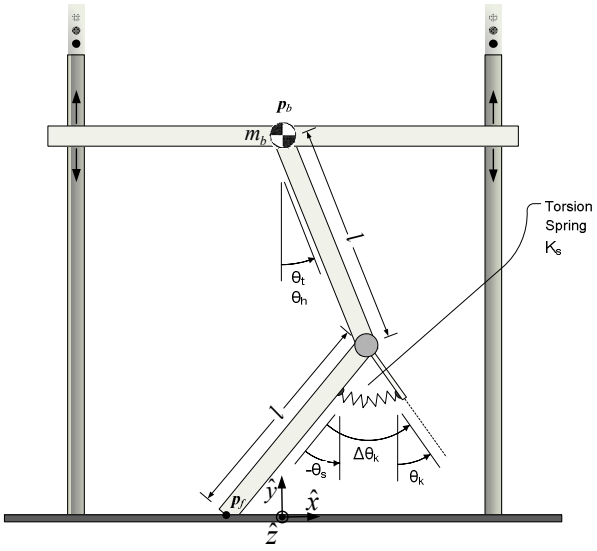

Fig. 2. Kinematic and dynamic model of the prototype leg.

yielding Olympic athletes capable of performing an 8 ft. high jump. To this end, intelligent control seeks to mimic some of nature's ability to learn and evolve by simplifying the details needed to manage the dynamic maneuver. Krasny and Orin demonstrated that an evolutionary algorithm with a modular controller was capable of finding solutions for complex behaviors in a quadruped such as a dynamically stable 3D gallop, high-speed turn, and running jump [13]. At the same time, evolution has been used to optimize the physical design of robotic systems under complex task-based constraints [14], [15]. The results are impressive and show that evolution is a fast and flexible design tool that performs well with complex physical constraints.

Naturally, one focus should be to apply an evolutionary algorithm to optimize the jump height of the prototype leg. Previous high jumps of the leg were a result of simply commanding full power to the leg during a crouch. However, biological evidence suggests that the timing of muscle contractions during a jump is critical, and so this paper will investigate if there are control strategies that can be used to obtain a better jump. Likewise, Bobbert [8] found that jump performance was highly dependent upon the stiffness of the skeletal muscle. This will be explored in the prototype leg by allowing an evolutionary algorithm to determine the stiffness and gear ratio of the actuators at both joints.

The organization of this paper is as follows. First a model of the actuators and prototype leg will be given followed by a brief explanation of the genetic algorithm and it's fitness function. Next, the control parameters are evolved and then the actuator parameters. Lastly, a summary and description of future work is presented.

II. Leg and Actuator Model

A simplified model of the prototype leg is depicted in Fig. 2. The total mass of the leg m_b is $4.019\ kg$ and represents the combined mass of the body, thigh, shank, and actuators. For the simplified model, this is shown by a point mass located on the body coincident with the hip axis. The length of each leg segment l is $0.1397\ m$. For the series-elastic actuation at the knee, the knee motor adjusts the rest position of the torsion spring by actuating θ_k. The torque applied to the shank τ_s is a function of the spring deflection $\Delta\theta_k = \theta_k - \theta_s$ and is expressed as $\tau_s = K_s \cdot \Delta\theta_k$. Since the thigh actuator is directly connected to the hip, the thigh torque τ_t can be determined from the actuator model.

A compact, yet detailed actuator model was developed to include the electrical and mechanical properties of the DC motors as well as the characteristics of the motor amplifiers. Combined, these properties are considered to accurately model the dominate characteristics of the actuators during a jump. The subscript m in the following equations indicate that the respective parameter should be evaluated for either the hip motor (h) or the knee motor (k). A list of the parameters for the Maxon motors and gears can be found in Table I.

TABLE I
Motor and Gearbox Parameters

Parameter	Units	Knee Motor Model EC 40	Hip Motor Model EC 32
Mass	kg	0.503	0.284
Combined Rotor and Gearbox Inertia (J_m)	$kg{\cdot}m^2$	9.44×10^{-6}	3.00×10^{-6}
Combined Rotor and Gearbox Damping (B_m)	$\frac{kg{\cdot}m^2}{s}$	8.60×10^{-6}	5.10×10^{-6}
Forward Gear Efficiency (η_{f_m})	–	0.75	0.70
Torsion Spring Stiffness (K_m)	$\frac{Nm}{rad}$	16.54	–
Torque Constant (K_{τ_m})	$\frac{Nm}{A}$	0.043	0.040
Winding Resistance (R_m)	Ω	1.69	5.50
Gear Ratio (n_m)	–	66 : 1	33 : 1

The motor amplifiers (Advanced Motion Controls model ZB12A8) limit the maximum obtainable current in the motor armature circuit to I_{max} ($7.5\ A$ for hip and $12.0\ A$ for knee). Also, the commanded current i_c is only realized in the armature circuit as long as the voltage required to do so does not surpass the supply voltage V_{max} (48V). When the motor velocity surpasses the critical velocity $\dot{\theta}_m^\star$ expressed as

$$\dot{\theta}_m^\star = \frac{V_{max} - R_m i_c}{K_{\tau_m}}\ , \tag{1}$$

the damping effect of the back-emf voltage begins to restrict the armature current. With these constraints in place, the governing second-order motor equation can be expressed as

$$\bar{\tau}_m = J_m \ddot{\theta}_m + \bar{B}_m \dot{\theta}_m + \frac{\tau}{\eta \cdot n_m}\ , \tag{2}$$

where τ represents a joint torque ($\tau = \{\tau_h, \tau_k\}$) and the effective motor torque $\bar{\tau}_m$ and damping $\bar{B}_m$ are given by

$$\bar{\tau}_m = \begin{cases} K_{\tau_m} i_c & \text{when } \dot{\theta}_m \le \dot{\theta}_m^\star \\ \frac{V_{max} K_{\tau_m}}{R_m} & \text{when } \dot{\theta}_m > \dot{\theta}_m^\star \end{cases} \tag{3}$$

$$\bar{B}_m = \begin{cases} B_m & \text{when } \dot{\theta}_m \le \dot{\theta}_m^\star \\ B_m + \frac{K_{\tau_m}^2}{R_m} & \text{when } \dot{\theta}_m > \dot{\theta}_m^\star\ . \end{cases} \tag{4}$$

The approximate gearbox efficiency η_m is expressed by $\eta_m = \eta_{f_m}$ when $\dot{\theta}_m \tau_m \geq 0$ and $\eta_m = 1/\eta_{b_m}$ when $\dot{\theta}_m \tau_m < 0$. A manufacturer's backdrive efficiency η_{b_m} could not be assigned for the Maxon planetary gearheads, so the model will be evaluated at $\eta_{b_m} = \eta_{f_m}/2$.

The kinematic equations for the leg can be derived from the two points, $\boldsymbol{p}_f$ and $\boldsymbol{p}_b$, depicted in Fig. 2. The point $\boldsymbol{p}_f = [x, 0]$, where x is the horizontal position of the foot, and $\boldsymbol{p}_b = [0, y]$, where y is the vertical height of the body.

The upward motion of the leg is a result of the joint torques creating a force on the body. The force vector $\boldsymbol{f}$ is defined as $\boldsymbol{f} = [f_x, f_y]^T$, where f_x is the horizontal force on the foot, and f_y is the vertical force. With the leg assumed to be massless in the simplified model, $\boldsymbol{f}$ is also the force vector on the body. Further, let the link torque vector $\boldsymbol{\tau} = [\tau_t, \tau_s]^T$. The force $\boldsymbol{f}$ is related to the link torque $\boldsymbol{\tau}$ by $\boldsymbol{f} = \boldsymbol{J}^{-T}\boldsymbol{\tau}$. Since the leg is constrained by vertical rails, only f_y affects its motion, which can be simplified as

$$f_y = \alpha\tau_t + \beta\tau_s \ , \tag{5}$$

where α and β are the following elements of the inverse Jacobian transpose

$$\alpha = \frac{-\cos(\theta_s)}{l\sin(\theta_t - \theta_s)} \ , \tag{6}$$

$$\beta = \frac{\cos(\theta_t)}{l\sin(\theta_t - \theta_s)} \ . \tag{7}$$

Finally, the dynamics of the rigidly connected hip actuator can be lumped into the dynamics of the body using the governing motor equation from Eq. 2. The result is a second-order differential equation describing the body height as follows

$$M\ddot{y} = \alpha\eta_h \left(n_h\bar{\tau}_h + C\dot{y}^2 - (\alpha n_h^2 \bar{B}_h)\dot{y}\right) + \beta\tau_s - m_b g \ , \tag{8}$$

where M combines the body mass and hip rotor inertia, and $C\dot{y}^2$ is the centripetal acceleration of the hip inertia (both reflected through the nonlinear transformation α) and are defined as

$$M = m_b + \eta_h n_h^2 \alpha^2 J_h \ , \text{ and} \tag{9}$$

$$C = \frac{n_h^2 J_h}{\sin(\theta_t - \theta_s)} \left(\alpha^2\cos(\theta_t - \theta_s) + \beta^2\right) \ . \tag{10}$$

Dynamic simulation was implemented in MATLAB® using simple Newton-Euler integration with a 0.1 ms time step.

III. The Adaptive Evolutionary Algorithm

The best set of control and actuator parameters is found using a genetic algorithm (GA). This work used the Genetic Algorithm and Direct Search Toolbox 1.0.1 provided by MATLAB®. The genetic algorithm is employed to optimize a simulated jump while meeting certain physical constraints. Specifically, it optimizes a scalar fitness function that is proportional to the height of a jump but subject to fitness penalties based on physical limitations. Certain refinements to the algorithm were made to help prevent the search from converging to the many local optima that riddle the parameter space. This was accomplished by adjusting the crossover fraction $p_c = \{p_{c1}, p_{c2}\}$ $(p_{c1} < p_{c2})$ and mutation rates $p_m = \{p_{m1}, p_{m2}\}$ $(p_{m1} > p_{m2})$ during evolution when the diversity γ, or average Euclidean distance between the parameters of the solutions, was determined to shrink too early in the search process. This will be explained further once a few terms used by the GA are introduced.

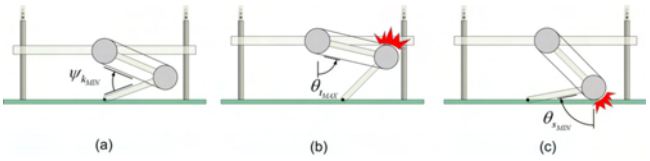

Fig. 3. Mechanical constraints enforced by the fitness function. In part (a) the leg is at a hard stop ($\Psi_{k_{MIN}} = 50.5°$), and in parts (b) and (c) the cable pulley at the knee has made contact with the body ($\theta_{t_{MAX}} = 70.5°$) and the ground ($\theta_{s_{MIN}} = -70.5°$), respectively.

First, an "individual" refers to a single solution ϕ^j comprised of a vector of parameters to be optimized. The set of S individuals represents the current working population $W(k)$, where k denotes the current generation. N is the total number of generations. The number of children in the next generation $W(k{+}1)$ created by crossover is $(S{-}\chi)p_c$; except for the elite individuals χ, the rest of the children in $W(k{+}1)$ are formed by mutation. If the diversity is less than γ and $k < N/2$, then the crossover fraction is decreased to p_{c1} and uniform mutation is performed with the larger mutation rate p_{m1} in order to promote exploration. Otherwise, the crossover fraction is set at p_{c2} and Gaussian mutation is performed with the smaller mutation rate p_{m2} to promote exploitation by randomly perturbing each parameter with a zero mean Gaussian distribution. As opposed to Zhang's adaptive genetic algorithm [16], this approach does not affect the final convergence because it stops adjusting the crossover and mutation when the solutions become too diverse or the search is nearing completion. The refinement can be thought of as a temporary tradeoff of the algorithm's exploitation ability for more exploration when the population diversity becomes small. Without this technique the algorithm had difficulty finding viable solutions in a reasonable number of trials. Finally, note that 30 trials of the GA were run for each optimization problem, with 200 generations per trial, and a population size of 150 individuals per generation.

Fitness Function

The criteria used in the fitness function are critical in achieving the desired behavior. By introducing weights based on different rules, certain solutions can be either encouraged or discouraged. As with any robotic mechanism, the prototype leg can only operate safely within a subset of the leg's joint space. Figure 3 depicts the three configurations where the leg is at the boundary of the allowable joint space. All three cases are considered unacceptable and are penalized by the fitness function. In addition, foot slip with the prototype leg is undesirable and as such can be penalized by the fitness function. The dynamics of slip are not simulated, but the

TABLE II

RANGES FOR EACH EVOLVED PARAMETER FOR THE JUMP.

Parameter	Description	Range
y_{b_0}	Initial Body Height	$[0.01, 0.28]\ m$
t_m	Time Stamp	$[0.01, 0.75]\ s$
i_h	Hip Current	$[-7.5, 2.0]\ A$
i_k	Knee Current	$[-2.0, 12.0]\ A$

presence of slip can easily be detected by inspection of the foot force at the ground. If the resulting foot force ($\boldsymbol{f}$) is outside of the arc defined by the friction triangle ($2\tan^{-1}\mu$), the foot will slip. The static coefficient of friction used is $\mu = 0.51$, which is close to the value for the aluminum foot of the prototype on the rubber surface of the ground.

The fitness function f is ultimately what is being maximized by the genetic algorithm. The primary component of the fitness function is h, the height of a jump using parameters ϕ^j. The complete fitness function is given as

$$f = (f_1 \cdot f_2 \cdot f_3 \cdot f_4) \cdot h \qquad \text{where } 0 \leq f_i \leq 1\ . \quad (11)$$

The weight f_1 is used to penalize the solutions that slip and the other three $f_2 \ldots f_4$ are used to penalize solutions that exceed the joint limits. They are computed as

$$f_i = \left(1 - \frac{T_i}{T}\right)\ , \quad (12)$$

where T_i is the time the leg slipped or exceeded the joint limit and T is the total time of the entire jump. It is possible for more than one condition to be broken during a simulated jump, in which case the height is heavily penalized. Since allowing the leg to simulate past these joint limits or when the foot would otherwise slip often resulted in higher jumps, care was taken to assess the penalties so that these individuals could still contribute their genetic material to the population. Much like a simple proportional controller, this method assigns a penalty that is proportional to the amount of time spent slipping or outside the allowed joint space. The results will show that the joint trajectories of the best solutions temporarily converge to a few of the joint limits, but never exceed them, therefore realizing the best jump within the constraints of the joint space and with minimal slip.

IV. EVOLVING A BEST JUMP CONTROLLER

Work by Curran [17] studied how the physical parameters of the SEA could be optimized to create the highest jump. However, to simplify the analysis, the motors were simply commanded maximum current for the entire jump. This section will explore the effects of varying the current commanded to each motor with time by introducing a current profile. In general, a current profile commands a set of currents i_{m_j} at time t_{m_j} to motor m and is described by

$$\boldsymbol{i}_m = [i_{m_0}(0), i_{m_1}(t_{m_1}), \ldots, i_{m_n}(t_{m_n})]\ . \quad (13)$$

The n current commands are combined with the $n-1$ time stamps to give the current profile. Notice that one less time parameter is needed because it is always necessary to command a current at time $t = 0$.

TABLE III

EVOLVED PARAMETERS FOR THE JUMP WITH NO CURRENT PROFILE.

	Parameters		
Height	y_{b_0}	$i_{h_0}(0)$	$i_{k_0}(0)$
$0.6756\ m$	$0.119\ m$	$-7.50\ A$	$12.0\ A$

A comparison will be made between a jump that is allowed a very simple current profile ($n = 1$) and one with no current profile ($n = 0$). First, only the mechanical constraints of the joint space will be enforced by the fitness function, and slip will be ignored so that the resulting behaviors are independent of the surface friction. The foot will be positioned directly beneath the hip axis, and the initial body height and current profiles will be found using the genetic algorithm. For the case where $n = 0$, the evolvable parameters are:

$$\phi_1 = \left[y_{b_0},\ i_{h_0},\ i_{k_0}\right]\ , \quad (14)$$

where y_{b_0} is the initial body height. For the case where $n = 1$, the evolvable parameters become:

$$\phi_2 = \left[y_{b_0},\ i_{h_0},\ t_{h_1},\ i_{h_1},\ i_{k_0},\ t_{k_1},\ i_{k_1}\right]\ . \quad (15)$$

The search range for each parameter is given in Table II and was determined heuristically after performing multiple simulations. The body position y_{b_0} and current range i_m are a combination of physical limitations and experimental tuning. In particular, large motor currents that pulled the leg into the ground produced poor results and were removed from the search space.

Evolutionary results for the case with the current profile (parameters of Eq. 15) consistently gave two distinctly different solutions with nearly identical fitness depending upon the random initialization of the individuals in the first population. The final evolved values and resulting jump height of the parameters in Eq. 14 are listed in Table III, and the evolved values and jump heights of the two modes found from Eq. 15 are listed in Table IV. Simulation results of the three solutions are given in Fig. 4.

The most defining characteristic of the two modes generated with the current profile are the different starting heights of the body y_{b_0}. One starts standing nearly straight up at $27\ cm$, while the other is crouched almost as low as possible. Not only did the current profile allow the GA to find these two interesting modes, it also produced jumps where the distance of the foot above the ground at the top of flight (TOF) was approximately 20% higher than the case without a current profile. For the crouch jump (no current profile), evolution determined that the body must start at $y_{b_0} = 0.119\ m$ above the ground and apply maximum current to each motor. At this starting height, the body is in the configuration depicted in Fig. 3a, which is at one of the physical limits of the leg's joint space. In this case, starting at a lower body height would result in a higher jump, but is not feasible. As was stated earlier, this shows the ability of the fitness function to converge to a solution that both is optimal and enforces the mechanical constraints of the leg.

TABLE IV

EVOLVED PARAMETERS FOR THE JUMP WITH A CURRENT PROFILE.

	Parameters						
Height	y_{b_0}	$i_{h_0}(0)$	t_{h_1}	$i_{h_1}(t_{h_1})$	$i_{k_0}(0)$	t_{k_1}	$i_{k_1}(t_{k_1})$
0.7587 m	**0.267 m**	-0.06 A	0.165 s	-7.50 A	-0.04 A	0.175 s	12.0 A
0.7576 m	**0.127 m**	1.470 A	0.099 s	-7.50 A	9.77 A	0.103 s	12.0 A

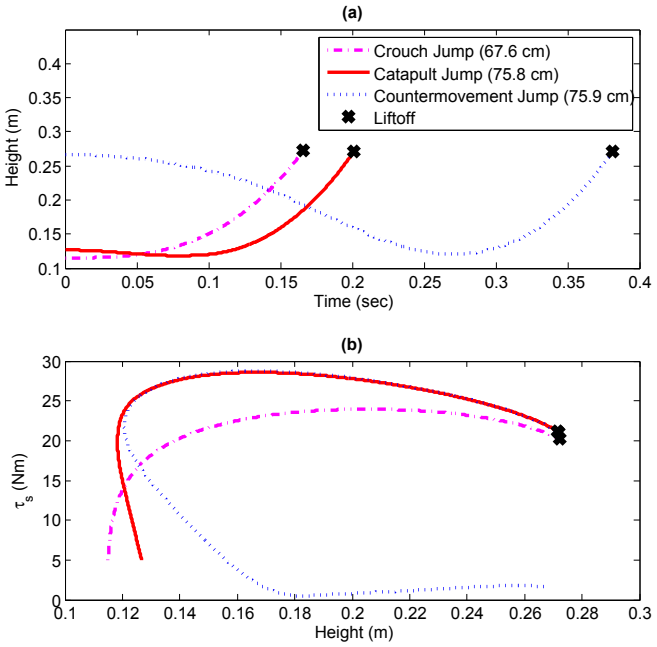

Fig. 4. Simulation results for the three solutions found by the GA before liftoff. The catapult jump and countermovement jump were allowed a simple motor current profile, while the crouch jump was not. Note that the plot of τ_s vs. y_b is useful for comparing the crouch and catapult modes.

In fact, the height of the body in all three solutions can be observed in Fig. 4a to drop down to, but never go beneath, this physical limit.

The two distinctly different solutions with nearly identical jump heights were an unexpected result of evolving a jump with a simple current profile. One solution found by the GA was to start the leg standing nearly upright and perform what is known in plyometrics to be one of the most explosive movements, a countermovement jump [18]. A countermovement jump (CMJ) begins in an upright stance and is depicted in Fig. 5. First the legs are relaxed temporarily to allow the body to fall toward the ground. Moments later, the leg explodes into a jump. The energy of the falling body is stored in elastic elements of the leg, then delivered before liftoff, causing larger forces during the jump. In exercise physiology, this is termed the stretch and shortening cycle and is one of the underlying mechanisms of plyometrics [1]. All of these significant indicators of a CMJ are present in Fig. 4 a-b. The spring-recoil occurs when the motors apply full power while the body is still falling and is ultimately what produces the stretch phase of the cycle. Another variation of the stretch and shortening cycle, similar to that observed in jumping insects, occurs with the other solution.

Referred to as the catapult jump in Fig. 4, the second

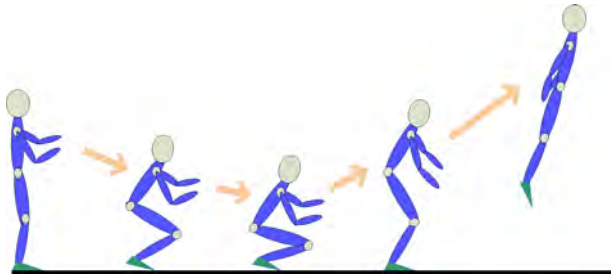

Fig. 5. Illustration of a Countermovement Jump.

jump begins in a crouch slightly higher than the simple jump evolved with no current profile. Instead of immediately applying full motor power as in the crouch mode, the current profile momentarily redistributes the joint torques by retracting the thigh and further flexing the knee spring. The body drops slightly as its weight is put onto the knee, and the elastic element builds up additional torque to counter gravity. Then seamlessly, both motors explode with full torque, and the body quickly begins to accelerate upwards with a larger torque than the crouch jump (Fig. 4 b). This motion is very similar to the catapult action seen in a grasshopper jump [19], [20]. First, with help from the two front legs, the insect leans back onto the hind legs, and the body drops slightly just as in Fig. 4. Then, the insect quickly thrusts upwards with a larger force and releases the extra elastic energy stored during the initial contraction. This is another variation of the stretch and shortening cycle discussed earlier. In the catapult jump, the stretch is a result of an active redistribution of torques, rather than the recoil of the falling body in the countermovement jump. The CMJ used only 32.25 J of energy, while the catapult jump used 37.32 J. The difference in energy is nearly the same as the change in potential energy of the body for the CMJ from the initial stance to the recoil during the crouch. Therefore, without the kinetic energy of the falling body, the catapult jump must generate this additional energy with the motors.

Eliminating Slip

In all three cases, the no-slip condition was not enforced by the fitness function to allow for a raw comparison of jump performance with and without a current profile. As a result, the crouch jump would have slipped 67.5% of the time, the catapult jump 95.6% of the time, and the countermovement jump 58.0% of the time. However, by temporarily ignoring slip, the GA was able to quickly find two interesting jump modes using a very simple current profile. Nevertheless, in keeping with the real constraints of the prototype leg further evolution was done where the no-slip condition was enforced by the fitness function. In addition to the body's starting height, the initial horizontal foot position was added as an

TABLE VI

EVOLVED SEA PARAMETERS FOR THE BEST JUMP.

	Parameters					
Height	y_{b_0}	ρ	n_h	n_k	K_t	K_s
1.1325 m	0.120 m	1	77.62	77.51	54.54 Nm/rad	54.74 Nm/rad

TABLE V

RANGES FOR EACH EVOLVED PARAMETER FOR THE SEAS.

Parameter	Definition	Range
y_{b_0}	Initial body height	$[0.01, 0.28]$ m
ρ	SEA at hip ($\rho = 1$), DDA at hip ($\rho = 0$)	$\{0, 1\}$
n_h	Gear ratio for hip actuator	$[5:1, \ 1000:1]$
n_k	Gear ratio for knee actuator	$[5:1, \ 1000:1]$
K_t	Spring stiffness for hip SEA (when $\rho = 1$)	$[1, 500]$ Nm/rad
K_s	Spring stiffness for knee SEA	$[1, 500]$ Nm/rad

evolvable parameter to assist in the search for a slip-free solution. Different foot positions allow the joint torques to contribute more force in the vertical direction and less in the horizontal direction, thus controlling slip. Unlike the previous problem, the evolutionary search only found the CMJ to be the optimal jump mode, but this was expected since it had the least amount of slip in the previous problem. The jump resulted in nearly the same 20% increase in jump height (distance of the foot above the ground at TOF) with slip occurring for only 4.27% of the jump. Slip was virtually eliminated when the size of the current profile was increased to $n = 4$.

V. EVOLVING ACTUATORS FOR A BEST JUMP

An analysis of liftoff performed by Curran [17] suggested that replacing the direct-drive actuator (DDA) at the hip with an SEA would greatly improve the jump height. To investigate this further, the GA here was allowed to evolve either a DDA or an SEA at the hip using the binary parameter ρ. The gear ratio and spring stiffness of the DDA and SEA are also left to the GA to be found; however, the spring stiffness at the hip K_t will be ignored when $\rho = 0$ (no SEA). Furthermore, to fully explore the optimization power of the GA, the parameters of the SEA at the knee will also be evolved. As was done in the last section, the no-slip condition will not be enforced to allow for a raw comparison of jump performance independent of the surface friction. The foot will be fixed to be directly beneath the hip axis, but the initial body height y_{b_0} will be left to the genetic algorithm to determine; however, the physical constraints on the joint space will be enforced by the fitness function. Finally, the motors will be commanded full current at $t = 0$ in order to compare the solutions with the best solution from Table III. To summarize, the evolvable parameters are:

$$\phi_5 = \Big[y_{f_0},\ \rho,\ n_h,\ n_k,\ K_t,\ K_s \Big] \ . \tag{16}$$

The search range for each parameter is given in Table V and was determined heuristically after performing multiple simulations. It is important to note that the motor of the SEA at the hip is that of the SEA at the knee. That is, when $\rho = 1$, the parameters of the hip motor become $K_{\tau_h} = K_{\tau_k}$, $R_h = R_k$, $J_h = J_k$, $B_h = B_k$, and $\eta_h = \eta_k$.

The final evolved values of Eq. 16 are listed in Table VI. Note that the solution has an SEA at the hip ($\rho = 1$) and resulted in a dramatically larger jump height than the original parameters. In fact the actuators evolved here contributed approximately 215% more to the jump height (distance of the foot above the ground at TOF) than the original actuators.

An important attribute of the optimal solution is that the two SEAs have nearly identical parameters. That is, the gear ratio and spring stiffness of the hip SEA is very close to that of the knee SEA. The other defining characteristic of the best solution was that it was completely slip-free, even though the no-slip condition was not enforced. In fact, evolution of the same parameters of ϕ_5 in Eq. 16 when the slip condition was enforced consistently gave the optimal solution of Table VI as the best solution. This means that identical SEAs at both joints with the parameters given in Table VI will result in the highest jump, which is also slip-free. Other suboptimal, but still impressive, solutions found on different trials did not have identical hip and knee SEA parameters and encountered brief periods of slip. Therefore, it is reasonable to assume that the complete elimination of slip is a result of having SEAs at both joints with nearly identical gear ratios and spring stiffnesses.

VI. SUMMARY AND FUTURE WORK

In this study, the genetic algorithm (GA) was presented and was used to optimize a jump while meeting certain physical constraints. Specifically, it evolved a current controller that discovered interesting jump modes and evolved optimal SEA parameters. Certain refinements to the algorithm were made to help prevent the search from converging to the many local optima that riddle the parameter space. This was accomplished by adjusting the crossover and mutation rates during evolution when the diversity of the solutions was determined to shrink early in the search process. The higher mutation rates could be tolerated because the risk of losing good solutions was minimized through an elitist strategy.

Like skeletal muscle, the timing of the control inputs was found to be crucial in creating the highest jump. The GA found that a simple current profile could produce jump heights that were approximately 20% higher than jumps when just full motor current was commanded. The current profile produced two new jump modes that resembled the explosive countermovement jump performed in plyometric training and the catapult jump performed by insects. Both modes developed additional torque in the spring by momentarily compressing it before exploding into the jump. The larger torque and additional spring energy result in higher

liftoff velocities. In exercise physiology, this is termed the stretch and shortening cycle and is one of the underlying mechanisms of plyometrics. When the no-slip condition was enforced and the foot position allowed to vary, the GA found the countermovement jump to be the optimal mode of control. In fact, it was able to reach nearly the same height as the optimized jump when the no-slip condition was not enforced.

Evolving parameters for the hip and knee actuators proved to be an elegant solution to the problem of maximizing jump height. Similar to Bobbert's findings of the dependence of human jump performance on elasticity in skeletal muscle [8], the spring stiffness was found here to have a large impact on the jump performance. The GA was able to dramatically increase the jumping height and provide a completely slip-free solution by placing nearly identical SEAs at both joints. In fact, the actuators evolved by the GA resulted in a jump that was approximately 215% higher than the original actuators. Future jumping machines would benefit from having SEAs at both joints.

Although this approach has generated some impressive solutions, there is still more work that could be done. First, the control solution found here that generates the countermovement jump should be tried in hardware and compared to the crouch jump. Also, experimental results indicate that the first few jumps of continuous hopping increase in height. It is highly likely that genetic optimization would identify this behavior and exploit it to produce a set of extremely high jumps. However, in order to avoid damaging the actual hardware, care should be taken to minimize the number of jumps as well as to confine the behavior of each jump. This could be accomplished by porting the best control modes discovered by the GA in simulation to the actual hardware and allowing the last stages of learning to proceed with a GA or alternate strategy capable of online learning.

Finally, because full autonomy may be necessary in high-speed robots capable of performing dynamic maneuvers, a thorough analysis of power and energy should be performed. It would be very revealing to allow the genetic algorithm to optimize jump height and power consumption. The total energy could be used to penalize the fitness function with an adjustable weight. Such an analysis and optimization will hopefully show that autonomy is possible and could give estimates for battery sizes and weights. The insight provided by this study in conjunction with future work will hopefully lay the foundation for future implementation of legged robots capable of autonomous high-speed locomotion and dynamic maneuvers.

VII. Acknowledgements

Support for this work was provided in part by Grant No. IIS-0535098 from the National Science Foundation to The Ohio State University, and through a teaching associateship with the Fundamentals of Engineering for Honors Program at The Ohio State University.

References

[1] D. A. Chu, *Jumping into Plyometrics*. Human Kinetics Publishers, 2 ed., 1998.

[2] A. Wilson, J. Watson, and G. Lichtwark, "A catapult action for rapid limb protraction," *Nature*, vol. 421, pp. 35–36, 2003.

[3] T. Roberts, "The integrated function of muscle and tendons during locomotion," *Comparative Biology and Physiology*, vol. 133, no. 4, pp. 1087–1099, 2002.

[4] T.J. Roberts, R.L. Marsh, P.G. Weyand, and C.R. Taylor, "Muscular force in running turkeys: the economy of minimizing work," *Science*, vol. 275, no. 5303, pp. 1113–1115, 1997.

[5] A. Hof, B. Geelen, and J. Van Den Berg, "Calf muscle moment, work and efficiency in level walking; role of series elasticity," *Journal of Biomechanics*, vol. 16, pp. 523–535, 1983.

[6] K. Kubo, Y. Kawakami, and T. Fukunaga, "Influence of elastic properties of tendon structures on jump performance in humans," *Journal of Applied Physiology*, vol. 87, no. 6, pp. 2090–2096, 1999.

[7] T.J. Roberts and R.L. Marsh, "Probing the limits to muscle-powered accelerations: lessons from jumping bullfrogs," *The Journal of Experimental Biology*, vol. 206, no. 15, pp. 2567–2580, 2003.

[8] M. F. Bobbert, "Dependence of human squat jump performance on the series elastic compliance of the triceps surae: a simulation study," *The Journal of Experimental Biology*, vol. 204, pp. 533–542, Jan. 2001.

[9] G. J. Ettema, "Mechanical efficiency and efficiency of storage and release of series elastic energy in skeletal muscle during stretch-shorten cycles," *The Journal of Experimental Biology*, vol. 199, no. 9, pp. 1983–1997, 1996.

[10] J. M. Remic III, "Prototype leg design for a quadruped robot application." Master's Thesis, The Ohio State University, Department of Mechanical Engineering, June 2005.

[11] S. Curran, "Real-time computer control of a high-performance, series-elastic, articulated jumping leg." Undergraduate Honors Thesis, The Ohio State University, Department of Electrical and Computer Engineering, Aug. 2005.

[12] B. T. Knox, "Evaluation of a prototype series-compliant hopping leg for biped robot applications." Undergraduate Honors Thesis, The Ohio State University, Department of Mechanical Engineering, June 2007.

[13] D. P. Krasny and D. E. Orin, "Evolution of dynamic maneuvers in a 3D galloping quadruped robot," in *Proc. of IEEE International Conference on Robotics and Automation*, Orlando, Florida, pp. 1084–1089, May 2006.

[14] O. Chocron and P. Bidaud, "Genetic design of 3D modular manipulators," in *Proceedings of the 1997 IEEE International Conference on Robotics and Automation*, pp. 223–228, 1997.

[15] I. Chen and J. Burdick, "Determining task optimal robot assembly configurations," in *Proceedings of the 1995 IEEE International Conference on Robotics and Automation*, pp. 132–137, 1995.

[16] Wei-Guo Zhang, Wei Chen, and Ying-Luo Wang, "The adaptive genetic algorithms for portfolio selection problem," *International Journal of Computer Science and Network Security*, vol. 6, pp. 196–200, January 2006.

[17] S. Curran, "Analysis and optimization of a jump for a prototype leg with series-elastic actuation." Master's Thesis, The Ohio State University, Department of Electrical and Computer Engineering, Aug. 2007.

[18] N. P. Linthorne, "Analysis of standing vertical jumps using a force platform," *American Journal of Physics*, vol. 69, pp. 1198–1204, November 2001.

[19] M. Burrows and O. Morris, "Jumping in a winged stick insect," *The Journal of Experimental Biology*, vol. 205, pp. 2399–2412, 2002.

[20] E. Tauber and J. M. Camhi, "The wind-evoked escape behavior of the cricket gryllus bimaculatus: integration of behavioral elements," *The Journal of Experimental Biology*, vol. 198, pp. 1895–1907, 1995.